Materials Science & Engineering A 729 (2018) 249–256

Contents lists available at ScienceDirect

Materials Science & Engineering A

journal homepage: www.elsevier.com/locate/msea

Tensile properties of spark plasma sintered AISI 316L stainless steel with unimodal and bimodal grain size distributions

B. Flipon[a], C. Keller[a,*], L. Garcia de la Cruz[b], E. Hug[b], F. Barbe[a]

[a] Groupe de Physique des Matériaux, CNRS UMR6634, Normandie Univ, UNIROUEN, INSA Rouen, Avenue de l'Université, 76800 Saint Etienne du Rouvray, France
[b] Laboratoire CRISMAT, CNRS UMR6508, Normandie Univ, 6 Boulevard du Maréchal Juin, 14050 Caen, France

ARTICLE INFO

Keywords:
Bimodal microstructure
Metals and alloys
Sintering
Grain size
Tensile properties

ABSTRACT

Powder metallurgy associated to spark plasma sintering was used to elaborate near full-dense samples of 316L austenitic stainless steel with unimodal or bimodal grain size distributions. To this aim, two different precursor powders were employed: a ball-milled one giving rise to ultrafine grains and a coarse one, as-received, for grains with conventional size. Sintered specimens were characterized in mechanical tension and their microstructure was revealed using transmission and scanning electron microscopy. Unimodal ultrafine grained samples show a large yield stress and a low ductility with a breakdown in the Hall-Petch relationship. For bimodal samples, a compromise between yield stress and ductility can be found. These features are then discussed in terms of strain mechanisms, grain size distribution and backstress. It is shown in particular that coarse grains contribute to enhance the ductility of the ultrafine grains matrix by modifying both the strain hardening mechanisms and the stress concentration areas.

1. Introduction

Grain Size (GS) reduction [1,2], especially in the ultrafine grain range, is known to improve the mechanical resistance of metallic alloys [3,4]. It also results in a severe loss in ductility [4,5] that might be detrimental concerning metal forming processes which involve large strains. To counterbalance this loss in ductility, several strategies can be employed. Among them, nanostructured metals with second phase precipitates, grain boundary engineering and bimodal microstructures give valuable results [6]. In nanostructured aged hardenable aluminium, the hard dislocation pinning precipitates enable a higher dislocation storage rate compared to conventional Al, which, in turn, improves the alloy capability to strain harden [7]. Nanocrystalline copper with engineered nano-twins also present an improved strain hardening. In this case twins hinder the dislocations motion and, as coherent interfaces, limit the detrimental effect on ductility observed in the case of a classical (incoherent) grain boundary [8]. However, these two elaboration processes are rather complex which can be problematic regarding their potential industrial applications. The third way of ductility improvement is based on the grain size distribution. Using large or Bimodal Grain Size Distributions (called BGSD in the following paragraphs), different grain populations are present which behave differently: the Fine or UltraFine Grain (FG or UFG) population will contribute to a large yield stress and the Coarse Grain (CG) one will improve ductility [9–11]. Such alloys with tailored microstructures may present a good compromise between enhanced yield stress and ductility.

Different processes are available in order to obtain bimodal microstructured alloys. A top-down approach consists in processing a bulk material to obtain the target microstructure. With such an approach, cold work and subsequent heat treatment(s) are suitable to generate bimodal microstructures [12,13]. In the case of austenitic stainless steel it involves strain induced martensite and reversed austenite after heat treatment [14–16]. However the control of the grain size distribution is hard and samples generally exhibit residual martensite [17]. Bottom-up approaches are mainly based on Powder Metallurgy (PM). In this case, commercial and/or ball-milled powders are used to obtain the final microstructure. The sintering step can be performed by several processes such as hot roll sintering [18–20] or hot isostatic pressing [10]. Elaboration of well-controlled BGSD microstructures is also possible through a route involving PM and Spark Plasma Sintering (SPS) [11,21–23]. Various blends of powders with different crystallite sizes can be sintered with a limited grain growth by means of SPS [24]. Grain size distributions can be controlled by varying both the crystallite size and the volume fraction of each grain size population.

For these bimodal samples, few works have been devoted to the analysis of the relationships between the grain size distribution and the mechanical properties [10,21,25,23]. Dirras et al. [10] and Tingaud

* Corresponding author.
E-mail address: clement.keller@insa-rouen.fr (C. Keller).

https://doi.org/10.1016/j.msea.2018.05.064
Received 7 May 2018; Received in revised form 18 May 2018; Accepted 18 May 2018
Available online 22 May 2018
0921-5093/

et al. [21] studied the influence of BGSD on deformation mechanisms after compression tests on Ni samples. Scanning electron microscopy alongside with electron backscattered diffraction have revealed a larger average strain in coarse grains clusters than in the UFG-matrix. *In-situ* transmission electron microscopy have confirmed the dislocation mediated process in BGSD (as also reported by X-Ray diffraction [10]) and have revealed UFG rotation during deformation [21]. For Ti alloy and 304L steel respectively, Wu et al. [25] and Park et al. [23] have shown by loading/unloading tensile tests and stress partitioning that strain hardening is also influenced by the backstress hardening arising from the BGSD.

The general objective of this paper is the experimental investigation of the influence of a BGSD on the mechanical properties in tension of AISI 316L samples obtained by spark plasma sintering. For this purpose, different batches of powders were prepared leading to six unimodal and six bimodal cases of study. In the bimodal configuration, both the volume fraction of each grain population and the size ratio were varied. The effects of the corresponding grain size characteristics on tensile properties were analyzed by focusing in particular on the long range stress interactions and on the deformation mechanisms.

2. Experimental procedure

As-received commercial powders of AISI 316L austenitic stainless steel correspond to single-crystalline powder grains of size 3 μm and to poly-crystalline powder grains with crystals mean size of 15 μm. In order to obtain ultrafine grains after sintering, the 3 μm commercial powder were ball-milled using a Fritsch Pulverisette 7 planetary mill at 500 rpm for 2 h. To prevent powder heating, the ball-milling was performed with 20 cycles of 5 min with a pause of 1 min between them and rotation direction was reversed from one cycle to another. The grinding bowls and balls are made of, respectively, tungsten carbide and austenitic stainless steel to avoid powder contamination. Around 24 g of powder and the same amount of ethanol (process control agent) were introduced in each bowl and 5 mm grinding balls were used with a 10:1 ball to powder mass ratio. With this procedure, three populations of grain powders were prepared and correspondingly three populations of grain sizes were expected to figure in the elaborated samples: UFG, FG and CG. Spark plasma sintering was conducted on a FCT System GmbH HD25. 50 mm graphite dies and around 50 g of powder were used to obtain 5–6 mm thick samples. Whatever the employed powder, the following SPS parameters were set: 1313 K for the dwell temperature and 50 MPa for the maximum pressure. SPS was realized under vacuum and heating and cooling rates were fixed at 100 K/min. The duration of the dwell plateau was set to 5 min. Both ball-milling and SPS conditions were optimized during a previous work [24].

To investigate the role played by the characteristics of the bimodal distribution, three series of samples were sintered. In the first series (S-I), 100% of ball-milled or as-received powders were used with different sintering times to obtain six different unimodal grain size distributions. The second series (S-II) was elaborated using a mixture of the ball-milled powder and CG powder. The third series (S-III) is similar to the second one except that the 3 μm as-received powder was employed instead of the ball-milled one. For these two series S-II and S-III, BGSD are expected. To analyse the role played by the volume fraction of each grain population –UFG, FG and CG– three different powder mass fractions (*i.e.* 75/25; 50/50; 25/75, expressed as %(U)FG/%CG) were tested for these bimodal samples.

The microstructure of the sintered specimens was characterized by Scanning Electron Microscopy (SEM) coupled with Electron BackScattered Diffraction (EBSD), density measurements, X-Ray Diffraction (XRD) and Transmission Electron Microscopy (TEM). After sample preparation by SiC manual polishing and electro-polishing with a A2 solution on a Lectropol-5 from Struers, SEM was performed on a Zeiss NVISION40 with an Oxford Instruments EBSD detector. EBSD scans with a step size providing at least 5 points per grain (along a given direction) were realized and analyzed using EDAX OIM analysis software. Density measurements were performed by the Archimede's method with a Kern laboratory balance (precision: 0.01 g). XRD have been performed using a Brucker D8 and X-Ray diffraction patterns obtained between 35° and 125° with 0.01° steps. Scanning Transmission Electron Microscopy (STEM) were realized on a JEOL ARM200F with 3 mm diameter samples etched at 20 V with a 10%-perchloric/90%-acetic acid solution.

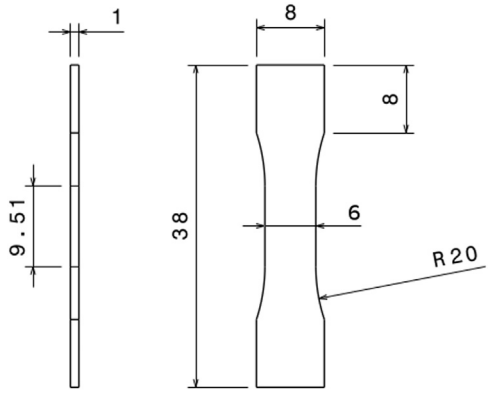

Fig. 1. Dog-bone tensile sample scheme. Dimensions are given in mm.

From the 50 mm diameter samples obtained after SPS, dog-bone tensile samples (gauge section: 6 × 1 mm - cf. Fig. 1) were extracted by electro-discharge machining to prevent any strong microstructure modification which can affect the mechanical properties [26]. After machining, the samples were then prepared by a careful polishing with SiC papers with a grit size down to 5 μm. Polishing was used to removed the residual surface rugosity induced by electro-discharge machining. Strain controlled uniaxial tensile tests were performed at $\dot{\varepsilon} = 2.\ 10^{-4}\ s^{-1}$ at room temperature (293 K) on a MTS Landmark 25 kN hydraulic machine with a 8 mm extensometer. For each sample obtained after SPS, at least 3 tensile tests were carried out in order to take into account the experimental scattering.

3. Results

3.1. Characterization of the sintered samples

Fig. 2(a) shows the microstructure observed by EBSD for a 75% UFG/25% CG mixture of the series S-II. A large grain size contrast is observed in agreement with the grain size distribution of the sample displayed in Fig. 2(b). In this figure, the grain size distribution of the UFG matrix obtained from the red delimited area in Fig. 2(a) is plotted together with the grain size distribution in a large grain size contrast area (blue delimited area in Fig. 2(a)) and the grain size distribution of the overall sample. For this series S-II, the measured characteristic sizes of the grain populations are approximately 0.3 μm (UFG) and 15 μm (CG). These characteristic sizes are also measured from EBSD maps for the other series: for S-III, the UFG population is replaced by a FG population with a mean grain size of 3 μm whereas for S-I, with unimodal grain size distribution, the mean grain size ranges from 0.3 μm to 15 μm, depending on the precursor powder (*i.e.* ball-milled or as-received) and the sintering time. For the three series, these extended EBSD analyses do not show any preferential grain orientations (maximum density pole of 2.2 and no texture pattern observed in pole figures), which ensures an isotropic mechanical behavior.

As summarized in Table 1, the sample densities are always larger than 94% with values closer to the theoretical one for BGSD specimens. However as illustrated in Fig. 3, for three samples - two unimodal ones (with grain sizes equal to 0.3 μm and 15 μm) and a bimodal one (75% of 0.3 μm-UFG and 25% of 15 μm-CG), this lower density is partly due to the presence of oxides. These second phases, already identified as rich